Jurnal Inovasi Teknologi Terapan
Vol. 04, No. 2, (2026) e-ISSN :3026-0213

Apparent Source-Level Efficiency of Internal Electric and External LPG Heating in a Laboratory Vacuum Evaporator

Erwin[1], Maulana Alfa Rizki[1], Syarif Abdullah[1], Slamet Wiyono[1]
[1]Universitas Sultan Ageng Tirtayasa, Serang
Email : erwin@untirta.ac.id
Received:4 Agustus 2026; Received in revised form: 8 Agustus 2026; Accepted: 9 Agustus 2026

Abstract

Background: Vacuum evaporation lowers boiling temperature, but performance depends on heat-source power and location, vacuum level, auxiliary demand, and the analytical boundary. This study compared an internally coupled electric resistance heater with an external LPG burner in the same laboratory vacuum evaporator using one non-replicated Water Boiling Test per configuration and 40 kg of water. Temperature, gauge pressure, water mass, reservoir temperature, and electrical variables were recorded every minute. The electric run lasted 367 min at 0.548 kW average source power; the LPG run lasted 300 min, consumed 0.80 kg fuel, and averaged 2.049 kW. LPG reached 65 °C at 35 min and evaporated 7.8 kg (0.0260 kg/min), whereas the electric heater reached 55 °C near the end and evaporated 2.4 kg (0.00654 kg/min). Apparent source-level efficiencies from a common sensible-plus-latent balance were 78.2% for electricity and 62.7% for LPG. A ±1 °C sensitivity changed these estimates by about ±1.39 and ±0.45 percentage points, respectively. Including vacuum-pump electricity reversed the system-level ordering. Because power, pressure, duration, and endpoints were not matched, the results describe two operating states rather than a causal heater-location effect.

Keywords: *Evaporation Throughput; Internal Resistance Heating; LPG Combustion; Source-Level Thermal Efficiency; Vacuum Evaporation*

Abstrak

Evaporasi vakum dapat menurunkan suhu didih, tetapi kinerjanya dipengaruhi oleh daya dan lokasi sumber panas, tingkat vakum, kebutuhan energi tambahan, serta batas analisis yang digunakan. Penelitian ini membandingkan pemanas resistansi listrik yang terkopel secara internal dengan pembakar LPG eksternal pada evaporator vakum laboratorium yang sama. Pengujian dilakukan menggunakan satu *Water Boiling Test* tanpa replikasi untuk setiap konfigurasi dengan 40 kg air. Suhu, tekanan ukur, massa air, suhu reservoir, dan variabel kelistrikan dicatat setiap satu menit. Pengujian menggunakan pemanas listrik berlangsung selama 367 menit dengan daya sumber rata-rata 0,548 kW, sedangkan pengujian menggunakan LPG berlangsung selama 300 menit, mengonsumsi 0,80 kg bahan bakar, dan menghasilkan daya sumber rata-rata 2,049 kW. Sistem LPG mencapai suhu 65 °C pada menit ke-35 dan menguapkan 7,8 kg air dengan laju penguapan 0,0260 kg/menit, sedangkan pemanas listrik mencapai 55 °C menjelang akhir pengujian dan menguapkan 2,4 kg air dengan laju 0,00654 kg/menit. Berdasarkan neraca energi sensibel dan laten yang sama, efisiensi semu pada tingkat sumber diperoleh sebesar 78,2% untuk listrik dan 62,7% untuk LPG. Analisis sensitivitas sebesar ±1 °C mengubah estimasi tersebut masing-masing sekitar ±1,39 dan ±0,45 poin persentase. Ketika konsumsi listrik pompa vakum dimasukkan ke dalam analisis, urutan kinerja pada tingkat sistem menjadi terbalik. Karena daya, tekanan, durasi, dan titik akhir pengujian tidak disamakan, hasil penelitian ini lebih tepat menggambarkan dua kondisi operasi yang berbeda, bukan menunjukkan pengaruh kausal dari lokasi sumber panas.

Kata kunci: Keluaran Evaporator; Thanan panas Internal; Pembakaran LPG; Efisiensi Thermal Sumber; Vacuum Evaporator

1. Introduction

Vacuum evaporation is widely used to concentrate foods, extracts, and fermentation streams while limiting thermal exposure. Lower pressure reduces saturation temperature and can improve retention of color, aroma, lycopene, phenolics, and other heat-sensitive attributes compared with atmospheric processing [1][2]. This is especially relevant for sugar-rich liquids, where temperature-time history affects browning, hydroxymethylfurfural formation, Maillard products, and flavor [3][4][5].

Evaporation performance is governed by pressure, temperature, heat-transfer area, liquid properties, residence time, and heat-input rate. Rotary vacuum evaporation of pineapple juice showed that scale-up can reduce water-removal performance when the heat-transfer-area-to-volume ratio falls [6][7]. Studies on honey, plant extracts, coconut water, dragon-fruit syrup, and arenga sugar similarly show that temperature and vacuum jointly affect water removal and product quality [8][9][10][11][12].

Energy demand remains a central constraint because evaporation requires both sensible heating and latent heat. Reviews of downstream bioprocessing identify evaporation and distillation as major energy users, while membrane and forward-osmosis preconcentration can reduce thermal load but introduce design complexity, concentration polarization, and fouling [13][14][15][16]. System-level analyses also show that energy-source choice and electrification can materially change cumulative energy use and emissions [17].

These constraints have encouraged heating methods that generate energy within or near the liquid. Ohmic systems create Joule heat through the product, whereas microwave systems couple electromagnetic energy to polar molecules. Vacuum-assisted ohmic evaporation has shown rapid heating and lower energy use than conventional vacuum evaporation in selected products, while models describe the coupled heat and mass transfer [18][19][20].

Microwave-vacuum studies likewise demonstrate that energy-delivery pathway matters. Heating and evaporation depend on dielectric properties, power density, vacuum level, and film thickness, with experimental evidence indicating that rapid thermal energy deposition is the dominant mechanism [21][22][23][24]. Electrodynamic and modular evaporator concepts further emphasize direct energy delivery, geometry, and mechanistic modeling as routes to process intensification and scale-up [25][26][27][28].

High evaporation rate, low specific energy, and high thermal efficiency are not necessarily achieved together. Power can also affect quality, crystallization, and process stability, so optimal conditions may occur below maximum input [29][30][31][32]. Heating configurations should therefore be compared with complementary indicators rather than maximum temperature or total mass loss alone.

External combustion and internal resistance heating create different heat-transfer pathways. With LPG, chemical energy reaches the liquid through flame-to-wall transfer, wall conduction, and wall-to-liquid convection, while hot gases, radiation, and exposed surfaces provide loss paths. An internal resistance element converts electricity to heat within the evaporator boundary and transfers it over a shorter distance to the water. Although this is not volumetric heating, it shares the process-intensification principle of locating heat generation close to the load. Vacuum and alternative concentration studies support the potential value of shorter thermal pathways and lower-pressure operation [33][34].

Most vacuum-evaporation studies focus on product quality, process optimization, or advanced heating, including banana syrup, honey, liquid sugar, grape juice, and alternative preconcentration routes [15][29][35][36][37][38]. A practical gap remains for small equipment: when an LPG burner evaporates water much faster than a low-power internal heater, the advantage may reflect higher installed power rather than higher energy efficiency.

An explicit energy boundary is required. Source-level efficiency compares sensible-plus-latent water energy with heater or fuel input; throughput is mass removed per time; specific source energy normalizes input by evaporated mass; and whole-system performance also includes auxiliaries. These metrics can rank configurations differently when warm-up, pressure, duration, or endpoints differ. Energy-integration studies likewise show that boundary choice and latent-heat reuse can alter conclusions [28][39].

Accordingly, this study compares an internally coupled electric resistance heater with an external LPG burner using minute-resolved Water Boiling Test data from the same laboratory evaporator. Temperature response, pressure behavior, water-removal rate, source energy, specific energy consumption, apparent first-law efficiency, and pump-energy sensitivity are evaluated with a common sensible-plus-latent balance. The working hypothesis was that internal electric heating would show a higher source-level water-energy ratio, whereas LPG would provide higher throughput because of its larger source power. Because source power, pressure, duration, and endpoints were not matched, the comparison is interpreted as two observed operating states rather than a causal heater-location experiment.

2. Materials and Methods

2.1 Research design and analytical boundary

A comparative laboratory test was conducted in one vacuum-evaporator vessel with two heating configurations. The internal configuration used a nominal 500 W spiral electric resistance heater, which converted electrical energy to heat within the evaporator boundary. The external configuration used an LPG stove beneath the vessel, requiring heat transfer from the flame through the vessel wall to the water. The primary efficiency boundary included only heat-source input and sensible-plus-latent energy gained by the water. Vacuum-pump electricity was analyzed separately because pump operation and pressure control differed between runs. All comparisons are therefore reported as properties of the recorded operating states rather than isolated heater-location effects.

2.2 Vacuum evaporator and instrumentation

The apparatus comprised a sealed evaporation vessel, internal spiral heater, external LPG stove, water-circulation pump, venturi vacuum generator, pressure controller, temperature sensors, electrical meters, and a digital balance. Heater voltage and current were recorded to calculate electrical power. The pressure controller cycled the pump during the electric run, whereas pump operation was continuous in the LPG record. Gauge-pressure data were converted to bar by dividing stored values by 1000. Water and reservoir temperatures were recorded every minute. Exported water temperatures were integer values, giving an effective analytical resolution of 1 °C. LPG consumption (0.80 kg) was obtained from endpoint cylinder weighing. Balance readability and calibration, pressure-sensor accuracy, and temperature-sensor calibration were not documented; therefore, derived LPG-energy and efficiency values are treated as point estimates with sensitivity analysis rather than formal uncertainty intervals.

2.3 Working fluid and test protocol

Water was used as the working fluid, with an initial mass of 40.0 kg for each run. After sealing the vessel and activating the vacuum system, the selected heat source was operated while temperature, gauge pressure, water mass, reservoir temperature, and electrical variables were recorded at 1-min intervals. The electric dataset contained 368 observations from 0-367 min; the LPG dataset contained 301 observations from 0-300 min. No interpolation or resampling was used to equalize duration. The shared graphical comparison is therefore 0-300 min, with 300-367 min representing an electric-only continuation. Initial/final temperatures were 31/55 °C for electricity and 32/65 °C for LPG; the LPG maximum was 67 °C. Final water masses were 37.6 and 32.2 kg, respectively.

Inspection of the complete datasets showed additional unmatched conditions. The electric run had a more negative mean gauge pressure, source powers differed substantially, and the tests ended at different times and temperatures. Warm-up slopes were therefore estimated over configuration-specific physical intervals: the first 60 min for electricity and the first 35 min for LPG, when the LPG record first reached 65 °C. Full-run mass and energy metrics use each run's actual endpoint. These distinctions prevent unequal duration from being mistaken for unequal sampling frequency or a matched experimental comparison.

Table 1. Experimental conditions and analytical boundaries for internal electric and external LPG heating.

Variable	Internal electric heating	External LPG heating	Analytical note
Heating location	Inside/closely coupled to water	Below vessel; open flame	Design contrast
Initial water mass	40.0 kg	40.0 kg	Common charge
Observations	368	301	1-min sampling
Duration	367 min	300 min	Shared 0-300 min; electric tail to 367
Temperature, initial/final/max	31/55/55 °C	32/65/67 °C	1 °C record

Variable	Internal electric heating	External LPG heating	Analytical note
Mean gauge pressure	−0.887 bar	−0.755 bar	Pressure unmatched
Heat-source input	548.2 W; 3.353 kWh	0.80 kg LPG; 10.244 kWh	0.80 kg endpoint fuel mass; balance accuracy unknown
Vacuum-pump behavior	Controlled cycling	Continuous in recorded data	Pump analyzed separately

2.4 Data preparation and quality control

Data were taken directly from the original workbook; rows without observation numbers were excluded and the native 1-min order was preserved. Heater and pump power were calculated as V×I, and pressure was converted to bar gauge. Series were checked for missing values and discontinuities; one final reservoir value in the electric dataset was missing and not imputed. Figures 1 and 3 use native records; Figure 2 uses a 5-min rolling mean only for clarity. Full-run statistics use actual durations, while direct trajectory comparison is limited to 0-300 min. The first 10 min were retained as pump-down behavior but excluded from stabilized-pressure summaries. No statistical outliers were removed. With no calibration records available, sensitivity analysis replaced formal uncertainty propagation.

2.5 Performance calculations

The average evaporation rate was calculated from the measured reduction in water mass:

$$\dot{m}_{ev} = (m_0 - m_f) / t$$

where m_0 and m_f are initial and final water masses and t is run duration. Electric-heater energy was obtained by trapezoidal integration of recorded power at 1-min intervals, yielding 3.353 kWh, essentially equal to average power multiplied by duration. LPG source energy was calculated as:

$$E_{LPG} = m_{LPG} \times LHV$$

where m_{LPG} is the recorded fuel consumption (0.80 kg) and LHV is 46.1 MJ/kg. LPG source energy was therefore 36.88 MJ (10.244 kWh). Average source power was source energy divided by duration, and specific source energy was source energy divided by evaporated-water mass. Because LPG balance accuracy was undocumented, 0.80 kg was treated as a point estimate. Holding useful-water energy fixed, LPG consumption would need to be about 0.642 kg, 19.8% below the recorded value, for its source-level efficiency to equal the electric estimate of 78.16%. This threshold is a sensitivity test, not a calibrated uncertainty interval.

Useful thermal energy was calculated as the sum of sensible heating of the initial water charge and latent energy associated with measured evaporation:

$$Q_{useful} = m_0 c_p (T_f - T_0) + m_{ev} h_{fg}$$

A constant water heat capacity of 4.186 kJ/kg.K and latent heat of 2257 kJ/kg were used as a transparent common basis. Terminal temperature was used in the primary balance; for LPG, the recorded maximum of 67 °C was also tested because it appeared in the original calculation. Apparent source-level efficiency was defined as $Q_{useful}/E_{source} \times 100\%$. The term apparent reflects omission of vessel and piping heat storage, condensate enthalpy, leakage, pressure-dependent property corrections, and formal uncertainty propagation. A ±1 °C sensitivity in ΔT changes sensible energy by ±0.167 MJ for the 40 kg charge, corresponding to about ±1.39 percentage points in electric efficiency and ±0.45 percentage points in LPG efficiency.

Vacuum-pump energy was integrated separately, giving approximately 2.598 kWh for the electric run and 2.797 kWh for LPG. These values were excluded from the primary source-level comparison but added in a system-level sensitivity analysis. This broader boundary illustrates how process duration and pressure-control strategy can alter overall energy performance even when the heat-source result is unchanged.

2.6 Statistical analysis

Because only one run was available per configuration, conventional between-group inference and run-to-run variability could not be estimated. Treating minute observations as replicates would be pseudoreplication because successive values are serially correlated. Analysis was therefore descriptive and trajectory-based. Mean, standard deviation, and range were calculated for temperature and pressure, including final-60-min and stabilized-pressure summaries. Warm-up rates were estimated by ordinary least squares over the first 60 min for electricity and 35 min for LPG; complete-run mass-loss slopes and R^2 values described mass trajectories. Performance metrics were compared using ratios and percentage differences, with no treatment-level p values or confidence intervals.

2.7 Research hypothesis and decision criteria

The working hypothesis was that internal electric heating would produce a higher source-level water-energy ratio because less energy is lost between generation and transfer to the water, while LPG would produce greater evaporation throughput because of its higher available source power. Internal heating was therefore evaluated primarily on energy utilization and LPG on throughput, but an adequate conclusion had to report both dimensions and explicitly acknowledge unmatched pressure, power, duration, and endpoints.

3. Results

3.1 Temperature response and heating dynamics

The internal-electric run warmed water from 31 to 55 °C over 367 min, with a full-run mean of 47.96 ± 4.83 °C. During the first 60 min, temperature increased at 0.245 °C/min (R^2 = 0.980); 45 °C was first reached at minute 52, 50 °C at minute 230, and 55 °C near the end. The final-60-min mean was 53.72 ± 0.67 °C. These decimal summaries average integer-degree observations and do not imply sub-degree sensor resolution.

LPG heating produced a faster temperature rise: 45 °C at minute 7, 60 °C at minute 23, and 65 °C at minute 35. The first-35-min slope was 0.803 °C/min (R^2 = 0.928), 3.28 times the electric warm-up slope. The maximum and terminal temperatures were 67 and 65 °C. All final-60-min records were 65 °C, indicating an apparent plateau within the 1 °C recording resolution rather than exact isothermal operation. The full-run mean was 63.66 ± 4.77 °C.

The faster LPG response does not itself establish higher efficiency. Average source power was 2.049 kW for LPG and 0.548 kW for electricity, a ratio of 3.74, while the warm-up-slope ratio was 3.28. The similar magnitudes are consistent with greater heat availability during the LPG run. Because power, pressure, endpoint, and warm-up windows differed, Figure 1 represents two operating trajectories, with direct visual comparison limited to the shared 0-300 min window.

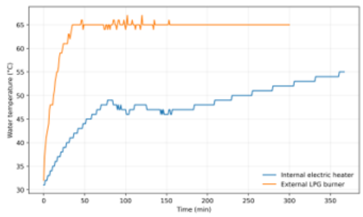

Figure 1. Water-temperature profiles at 1-min intervals. The shared comparison is 0-300 min; the electric run continues to 367 min. The 65 °C LPG plateau reflects the 1 °C recording resolution.

3.2 Vacuum pressure and pump behavior

Both runs reached negative gauge-pressure bands, but the levels were not matched. For electricity, full-run mean pressure was −0.887 ± 0.046 bar, the post-10-min mean was −0.890 ± 0.017 bar, and the final-60-min mean was −0.862 ± 0.004 bar. The pump was powered during 81.3% of the minute records, and integrated pump energy was approximately 2.598 kWh, confirming controlled cycling rather than continuous operation.

The LPG run operated at a less negative pressure: full-run mean −0.755 ± 0.038 bar, post-start-up mean −0.756 ± 0.027 bar, and final-60-min mean −0.740 ± 0.001 bar. Pump power was recorded throughout the run, averaging about 559.5 W and totaling approximately 2.797 kWh. Figure 2 displays a 5-min rolling mean, but the underlying sampling interval remained 1 min.

Pressure is therefore an important confounder. More negative pressure normally lowers saturation temperature, yet LPG operated at less negative gauge pressure while reaching higher temperature and evaporation rate. This pattern is consistent with the much larger LPG heat-input rate but cannot isolate heater location. Because pressure, source power, and endpoints were not matched, the observed efficiency difference is descriptive rather than causal.

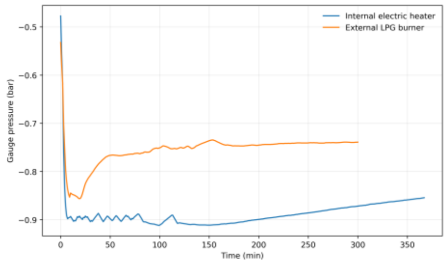

Figure 2. Five-minute rolling mean of vacuum gauge pressure from the native 1-min records. Electric operation was at a more negative pressure; direct comparison is limited to 0-300 min.

3.3 Water-mass reduction and evaporation throughput

Water mass decreased from 40.0 to 37.6 kg during the electric run, giving 2.4 kg removal and an endpoint evaporation rate of 0.00654 kg/min (1.09×10^{-4} kg/s). Linear regression of the complete mass series gave −0.00759 kg/min ($R^2 = 0.977$). The small difference from the endpoint rate reflects non-uniform mass loss over time; the high R^2 describes the trajectory and does not represent experimental replication.

For LPG, mass decreased from 40.0 to 32.2 kg, giving 7.8 kg removal and an endpoint rate of 0.0260 kg/min (4.33×10^{-4} kg/s). Complete-run regression yielded −0.02714 kg/min ($R^2 =$ 0.920). On an endpoint basis, LPG removed 3.25 times more water and achieved a 3.98-times higher evaporation rate despite a run 67 min shorter.

Throughput should not be equated with efficiency. LPG source energy was about 3.06 times the electric input and average LPG source power was 3.74 times higher, close to the 3.98 evaporation-rate ratio. This supports higher installed heat-input rate as a major contributor to faster water removal, although unequal pressure, duration, and endpoints prevent a causal estimate of heater-location effects.

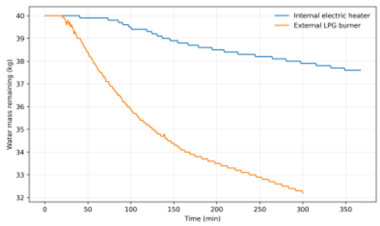

Figure 3. Water mass remaining at 1-min intervals. LPG showed greater observed throughput under the tested higher input power; the shared comparison is 0-300 min.

3.4 Source energy and specific energy consumption

Integrated electric-heater energy was 3.353 kWh (12.072 MJ), corresponding to 0.548 kW average source power and 1.397 kWh/kg of evaporated water. For LPG, 0.80 kg fuel at 46.1 MJ/kg gave 36.88 MJ (10.244 kWh), equivalent to 2.049 kW over 300 min and 1.313 kWh/kg.

Thus, the LPG point estimate used about 6.0% less source energy per kilogram evaporated, although the electric run had higher apparent source-level efficiency. The metrics differ because efficiency credits both sensible heating of the initial 40 kg charge and latent evaporation, whereas specific energy is normalized only by evaporated mass. The LPG values also depend directly on the endpoint fuel-mass estimate; the 0.642 kg equality threshold provides a robustness check without implying undocumented balance precision.

3.5 Apparent source-level thermal efficiency

For the electric run, useful water energy was 9.435 MJ: about 4.019 MJ sensible and 5.417 MJ latent. Relative to 12.072 MJ input, apparent source-level efficiency was 78.2%, leaving 2.637 MJ unaccounted for through equipment heat storage, environmental loss, property approximations, and measurement error. A ±1 °C change in ΔT shifts the efficiency estimate by approximately ±1.39 percentage points.

For LPG, useful energy based on the 65 °C terminal temperature was 23.130 MJ, including 5.526 MJ sensible and 17.605 MJ latent energy. Relative to the 36.88 MJ fuel-energy point estimate, apparent source-level efficiency was

62.7%. Using the 67 °C maximum increased it to about 63.6%. A ±1 °C change in ΔT shifts LPG efficiency by about ±0.45 percentage points. Fuel-mass uncertainty may be more influential: consumption would need to be about 0.642 kg, 19.8% below the recorded 0.80 kg, to equal the electric estimate.

Figure 4 summarizes the source-energy balance. Electricity converted a larger fraction of source energy into measured sensible-plus-latent energy, while LPG delivered more absolute useful energy because total input was larger. Unaccounted fractions were 21.8% for electricity and 37.3% for LPG. Hot gases, radiation, and exposed surfaces are plausible LPG loss paths, but they were not measured directly; the balance supports rather than proves this mechanism.

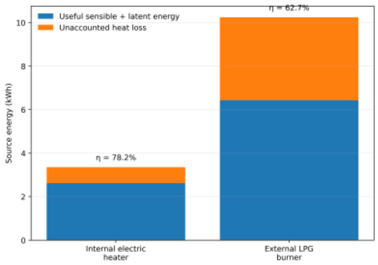

Figure 4. Source-level sensible-plus-latent energy balance. Internal electric heating converted a larger fraction of source energy into measured useful water energy.

3.6 System-level sensitivity including the vacuum pump

Including pump electricity broadened the boundary to approximate system performance. Heat-source-plus-pump energy was about 5.951 kWh for electricity and 13.042 kWh for LPG, giving useful-water-energy ratios of approximately 44.0% and 49.3%, respectively. The ordering reversed because the electric run lasted longer and accumulated substantial pump demand. Because controller logic and pressure set points also differed, these values remain descriptive rather than causal.

3.7 Integrated performance interpretation

Overall, LPG removed 7.8 versus 2.4 kg and had a 3.98-times higher endpoint evaporation rate while average source power was 3.74 times higher. Electricity had the higher apparent source-level water-energy ratio (78.16% versus 62.72%), whereas LPG had lower endpoint-specific source energy and a higher system-level ratio when pump electricity was included. Interpretation must retain three constraints: equal 1-min sampling but unequal durations, 1 °C temperature resolution, and an LPG energy estimate based on 0.80 kg endpoint fuel mass with undocumented balance uncertainty. The data therefore distinguish source utilization, installed heat-input capacity, and auxiliary demand without isolating heater location as the sole cause.

Table 2. Descriptive statistics and performance indicators derived from the minute-resolved dataset.

Metric	Internal electric heater	External LPG burner	Analytical qualification
Observations	368	301	1-min sampling
Duration	367 min	300 min	Shared 0-300 min
Temperature, mean ± SD	47.96 ± 4.83 °C	63.66 ± 4.77 °C	1 °C-quantized record
Warm-up slope	0.245 °C min−1; R^2=0.980	0.803 °C min−1; R^2=0.928	Different windows: 60 vs 35 min
Post-start-up pressure	−0.890 ± 0.017 bar	−0.756 ± 0.027 bar	Vacuum unmatched
Final 60-min temperature	53.72 ± 0.67 °C	65 °C throughout (1 °C resolution)	Plateau at recorder resolution
Evaporated water	2.4 kg	7.8 kg	LPG 3.25× more
Evaporation rate	0.00654 kg min−1	0.0260 kg min−1	LPG 3.98× higher
Mass-loss regression	−0.00759 kg min−1; R^2=0.977	−0.02714 kg min−1; R^2=0.920	Descriptive
Average source power	0.548 kW	2.049 kW	LPG 3.74× higher

Metric	Internal electric heater	External LPG burner	Analytical qualification
Source energy	3.353 kWh	10.244 kWh	Based on 0.80 kg endpoint fuel mass
Specific source energy	1.397 kWh kg−1	1.313 kWh kg−1	Endpoint-dependent
Useful water energy	9.435 MJ	23.130 MJ	Sensible + latent
Apparent source-level water-energy ratio	78.16%	62.72%	Point estimates; equality at mLPG ≈ 0.642 kg
Pump energy	2.598 kWh	2.797 kWh	Changes system result

4. Discussion

4.1 Internal heating and the source-level energy pathway

The principal source-level result was an apparent water-energy ratio of 78.2% for the internal-electric run versus 62.7% for LPG. This 15.4-percentage-point difference is physically consistent with the shorter heat-transfer path of the internal element. Electric resistance heat is generated within the evaporator boundary and transferred through the element surface to the water, whereas LPG energy must pass from flame to wall and then to the liquid, with additional loss paths through hot gases, radiation, and exposed surfaces. The measured unaccounted fractions, 21.8% and 37.3%, are consistent with this interpretation, although exhaust enthalpy and wall heat flux were not measured.

The mechanism is consistent with process-intensification studies in which heat is generated within or close to the product. Ohmic and microwave vacuum systems have been associated with faster heating, shorter processing, or lower energy demand than conventional indirect approaches [18][19][23][25]. The present resistance heater is not volumetric, but placing the conversion zone inside the evaporator removes the exposed flame-to-vessel stage. The agreement is therefore mechanistic rather than evidence that all internal-heating technologies have the same efficiency.

4.2 Why LPG produced much higher throughput

Higher source-level efficiency did not produce faster processing because evaporation capacity depends on useful heat rate as well as fractional efficiency. LPG supplied 2.049 kW, 3.74 times the 0.548 kW electric input. Applying the observed efficiencies gives useful rates of roughly 1.29 kW for LPG and 0.43 kW for electricity. This difference is consistent with the 3.28 warm-up-slope ratio and much of the 3.98 evaporation-rate ratio. LPG reached about 65 °C by 35 min, while the electric run reached 55 °C only near its 367-min endpoint.

Published direct-heating studies show the same dependence on applied power: microwave power and vacuum condition affect grape-juice evaporation, microwave power density governs sugar-solution heating, and voltage gradient affects ohmic-assisted vacuum evaporation [19][23][29]. The tested 548 W element therefore does not show that internal heating is inherently slow. A higher-capacity design should instead control surface heat flux, element area, immersion, circulation, and local boiling to avoid fouling or dry exposure.

4.3 Reconciling thermal efficiency and specific energy

The lower LPG source-level efficiency coexisted with a lower specific source energy: 1.313 versus 1.397 kWh/kg, about 6% lower. The apparent contradiction arises from different denominators. Source-level efficiency credits sensible heating of the full 40 kg charge plus latent evaporation; specific energy divides input only by evaporated mass. Because the electric run removed only 2.4 kg, its warm-up burden was distributed over less evaporated water, whereas LPG quickly completed warm-up and removed 7.8 kg.

This result demonstrates why specific-energy comparisons require a common endpoint. Evaporation trajectories can change with residence time, scale, heat-transfer area, and temperature [7][9][40]. Future tests should therefore terminate both configurations at the same condensate mass, concentration, or water-removal fraction. The present specific-energy values characterize these runs and should not be treated as technology constants independent of endpoint.

4.4 Vacuum pressure, boiling state, and auxiliary electricity

After start-up, electric operation was at a more negative mean gauge pressure (−0.890 bar) than LPG (−0.756 bar). The deeper vacuum supported evaporation at lower bulk temperature, while LPG maintained about 65 °C under a less negative pressure because of its higher heat input. Temperature and pressure therefore varied together, as in other vacuum-evaporation studies [6][12][29]. The efficiency difference cannot be assigned solely to heater location because thermodynamic states were not matched.

Auxiliary electricity further changes the evaluation boundary. Adding pump energy reduced the useful-water-energy ratio to about 44.0% for electricity and 49.3% for LPG, reversing the source-level ranking because the electric run was longer and pump demand was large relative to heater demand. Small venturi-based systems can therefore lose a source-level advantage through prolonged vacuum generation. Future comparisons should use matched pressure set points and controller logic and report both source-only and whole-system energy; process-control studies likewise emphasize coordinated control of energy, yield, quality, and stability [32][36].

4.5 Implications for temperature-sensitive products

The Water Boiling Test isolates thermal and hydraulic behavior, whereas the intended application includes sugar-rich liquids such as arenga sap. Low-temperature vacuum processing is attractive because cumulative thermal exposure influences color, HMF formation, aroma, and other quality attributes. Improved quality retention under vacuum has been reported for tomato paste, jujube jam, coconut sugar syrup, honey, and dragon-fruit products [1][8][11][33][41].

Internal electrical heating also offers direct power measurement and controllability through voltage/current monitoring and staged or proportional control. This is relevant because evaporation mode and energy input influence Maillard development, flavor, crystallization, antioxidants, color, and texture in sugar-rich products [2][4][5][30][38]. Follow-up tests with real sap should therefore measure energy and throughput together with °Brix, viscosity, HMF, color, reducing sugars, aroma, and fouling.

4.6 Design and scale-up implications

The engineering implication is not to replace LPG directly with the tested 548 W element, but to scale internal heating appropriately. At the observed source-level efficiencies, LPG delivered about 1.29 kW of useful heat; matching that useful rate would require roughly 1.65 kW electrical input, before scale-dependent losses. A staged design could use higher power during warm-up and lower power near boiling. Multiple low-surface-loading elements may distribute heat more uniformly and reduce local overheating compared with one compact high-flux element.

Scale-up must also account for geometry and product properties. Pineapple studies showed declining performance when heat-transfer area did not scale proportionally with volume, while thermophysical and dielectric properties changed with concentration and temperature [7][24]. Modular microwave work similarly emphasizes fluid level, geometry, and operating conditions [28]. For resistance heating, element area, clearance, immersion depth, circulation, cleanability, and insulation of the vessel, lid, and vapor lines should therefore be optimized together.

Process integration may provide further gains. Membrane or forward-osmosis preconcentration can reduce thermal load but remains constrained by fouling and selectivity [15][16]. Electrodynamic heating, vapor recompression, and integrated concentration illustrate options for direct energy delivery or latent-heat reuse [25][27][39]. At laboratory scale, immediate priorities are adequate internal power, insulation, condensate recovery, and pressure-based pump control.

4.7 Limitations and experimental priorities

The main limitation is the absence of independent replicate runs. Minute-by-minute observations describe each trajectory but are serially correlated and do not constitute treatment replication. Inferential comparisons would therefore be pseudoreplicated. Future work should use randomized independent runs per configuration to estimate repeatability and confidence intervals, with documented calibration and specifications for mass, temperature, pressure, electrical power, and LPG measurements.

Three additional limitations affect interpretation. First, sampling frequency was identical at 1 min, but LPG ended at 300 min and electricity at 367 min, so endpoint metrics did not share a termination criterion. Second, temperature was recorded at 1 °C resolution; the 65 °C LPG plateau therefore indicates no detectable change at that resolution. Third, LPG consumption was an endpoint value of 0.80 kg with undocumented balance accuracy, making LPG energy and efficiency point estimates. The 0.642 kg equality threshold is a sensitivity check, not a formal uncertainty interval. A decisive experiment should match source power and absolute pressure, use common initial conditions and endpoint, apply identical control logic, collect condensate independently, and use calibrated temperature and fuel-mass measurements. Equipment heat capacity, pressure-dependent properties, exhaust losses, and surface heat flux should also be measured where feasible.

Water also does not reproduce the viscosity, boiling-point elevation, foaming, fouling, or chemical reactions of concentrated sap. Product-dependent behavior has been reported for sour cherry, whey, and non-centrifugal sugar systems [5][42][43]. The next experiment should therefore repeat matched tests with arenga sap at defined initial and final °Brix and evaluate energy, throughput, and product quality together.

4.8 Scientific contribution

Within these limitations, the study separates three performance dimensions that are often conflated in small evaporators. LPG provided nearly four times the source power and much higher throughput; internal electric heating converted a larger fraction of source energy into measured water energy; and whole-system performance changed when vacuum-pump demand was included. Performance claims should therefore identify both the metric and the energy boundary rather than describing one configuration as universally better.

The resulting design hypothesis is testable: increasing internal-heater area and power while matching pressure and controlling auxiliary demand may retain the direct-transfer advantage while reducing the observed capacity deficit. This hypothesis is consistent with the direction of ohmic, microwave, and integrated vacuum-processing research but requires confirmation through replicated, power-matched experiments in the present apparatus and with the intended product.

5. Conclusions

Under the recorded operating conditions, LPG provided much higher throughput because its average source power was 3.74 times higher: it reached 65 °C at 35 min and evaporated 7.8 kg at 0.0260 kg/min, compared with 2.4 kg at 0.00654 kg/min for the 0.548 kW electric heater. However, the internal electric configuration had the higher apparent source-level water-energy ratio, 78.2% versus 62.7% for LPG. When vacuum-pump electricity was included, the system-level ratios became approximately 44.0% for electricity and 49.3% for LPG. Thus, the recorded data distinguish throughput, source-energy utilization, and auxiliary demand, but do not establish a causal heater-location effect because source power, pressure, duration, and endpoints were not matched.

The efficiencies are point estimates for two operating states. Replicated tests with matched source power, absolute pressure, initial conditions, and evaporation endpoint, plus calibrated temperature and LPG-mass measurements, are required before generalizing differences between heating configurations.

Acknowledgments
The authors gratefully acknowledge Universitas Sultan Ageng Tirtayasa for funding this research through the 2026 Internal Applied Research Grant.

References

[1] Devseren, E., Okut, D., Koç, M., Karataş, H., & Kaymak-Ertekin, F. (2021). Comparison of quality characteristics of tomato paste produced under atmospheric conditions and vacuum evaporations. *Anais da Academia Brasileira de Ciencias, 93 (1)*, Article e20200215. https://doi.org/10.1590/0001-3765202120200215
[2] Chen, Y. H., Chuah, W. C., & Chye, F. Y. (2021). Effect of drying on physicochemical and functional properties of stingless bee honey. *Journal of Food Processing and Preservation, 45 (4)*, Article e15328. https://doi.org/10.1111/jfpp.15328
[3] Altiok, D., Şen, L., & Altiok, E. (2022). Sweet pomegranate pekmez production: Effect of different production methods and activated carbon treatment on some quality parameters and 5-hydroxymethyl furfural formation. *Journal of Food Processing and Preservation, 46 (2)*, Article e16281. https://doi.org/10.1111/jfpp.16281
[4] Han, M., Zhao, H., Liu, Z., Liu, J., Liu, X., Hang, F., Li, K., & Xie, C. (2025). Color Development Characteristic and Kinetic Modeling of Maillard Reaction in Membrane-Clarified Sugarcane Juice During Vacuum Evaporation Process. *Foods, 14 (12)*, Article 2136. https://doi.org/10.3390/foods14122136
[5] Li, Q., Wang, Z., Gu, H., Ying, J., & Zhao, S. (2026). Changes in composition and flavor of non-centrifugal sugar after traditional Pan and vacuum evaporation processes.

Food Chemistry, 507, Article 148250. https://doi.org/10.1016/j.foodchem.2026.148250

[6] Leong, C. Y., & Chua, L. S. (2020). Optimization of concentrating process using rotary vacuum evaporation for pineapple juice. *Chemical Engineering Transactions, 78*, 7–12. https://doi.org/10.3303/CET2078002

[7] Chua, L. S., & Leong, C. Y. (2022). Optimization, Kinetic Studies, and Upscaling of Vacuum Evaporation for Pineapple Concentrates. *ACS Food Science and Technology, 2 (2)*, 331–336. https://doi.org/10.1021/acsfoodscitech.1c00425

[8] Mangku, I. G. P., Udayana, I. B. G., Hidalgo, H. A., Nicolas, A. R., & Fresnido, M. B. (2024). Vacuum evaporation optimization of Bali local honey for quality enhancement. *Food Research, 8 (6)*, 395–403. https://doi.org/10.26656/fr.2017.8(6).018

[9] de la Torre, J. J. M., Gragasin, M. A. C., & Caparino, O. A. (2023). Single effect evaporation of tender coconut water. *2023 ASABE Annual International Meeting*. https://doi.org/10.13031/aim.202300937

[10] Kulikova, N. E., Chernobrovina, A. G., Roeva, N. N., & Popova, O. Y. U. (2023). Evaporation as a Method for Obtaining Plant Concentrates [Исследование процесса выпаривания для получения концентратов из растительного сырья]. *Food Processing: Techniques and Technology, 53 (2)*, 335-346. https://doi.org/10.21603/2074-9414-2023-2-2438

[11] Susilo, B., Sutan, S. M., Hendrawan, Y., & Damayanti, R. (2021). Improving quality of dragon fruit (hylocereus costaricensis) syrup by processing with double jacket vacuum evaporator. *IOP Conference Series: Earth and Environmental Science, 924 (1)*, Article 012012. https://doi.org/10.1088/1755-1315/924/1/012012

[12] Erwin, E., Wiyono, S., & Yusuf, H. M. (2024). Investigation Effect of Liquid Arenga Sugar's Evaporation Temperature under Vacuum Pressure. *Journal of Research and Innovation in Food Science and Technology, 13 (2)*, 95-100. https://doi.org/10.22101/JRIFST.2023.382932.1432

[13] Xie, S., Li, Z., Zhu, G., Song, W., & Yi, C. (2022). Cleaner production and downstream processing of bio-based 2,3-butanediol: A review. *Journal of Cleaner Production, 343*, Article 131033. https://doi.org/10.1016/j.jclepro.2022.131033

[14] Szczygiełda, M., & Prochaska, K. (2020). Downstream separation and purification of bio-based alpha-ketoglutaric acid from post-fermentation broth using a multi-stage membrane process. *Process Biochemistry, 96*, 38–48. https://doi.org/10.1016/j.procbio.2020.05.026

[15] Tavares, H. M., Tessaro, I. C., & Cardozo, N. S. M. (2022). Concentration of grape juice: Combined forward osmosis/evaporation versus conventional evaporation. *Innovative Food Science and Emerging Technologies, 75*, Article 102905. https://doi.org/10.1016/j.ifset.2021.102905

[16] Ma, Z., Noor, I. I., Wang, X., Ren, Y., Wang, J., Wang, Q., Gao, J., Gao, X., & Liu, H. (2024). A comprehensive review on the recent advances in membrane-based processes for fruit juice concentration. *Food and Bioproducts Processing, 145*, 42–66. https://doi.org/10.1016/j.fbp.2024.02.010

[17] Checkoway, S. M., Lewis, G. M., & Keoleian, G. A. (2024). Carbon and Energy Footprinting across Archetypes for U.S. Maple Syrup Production. *Environmental Science and Technology, 58 (49)*, 21499–21509. https://doi.org/10.1021/acs.est.4c03067

[18] Aslam, R., Shafiq Alam, M., Kumar Vishwakarma, R., & Maqsood, S. (2024). Ohmic heating assisted vacuum evaporation chamber: Finite element analysis and evaluation of parameters for processing of amla juice. *Computers and Electronics in Agriculture, 224*, Article 109249. https://doi.org/10.1016/j.compag.2024.109249

[19] Tunç, M. T., Akdoğan, A., Baltacı, C., Kaya, Z., & Odabaş, H. B. (2022). Production of grape pekmez by Ohmic heating-assisted vacuum evaporation. *Food Science and Technology International, 28 (1)*, 72–84. https://doi.org/10.1177/1082013221991616

[20] Icier, F., Cokgezme, Ö. F., Döner, D., Bayana, D., Kaya, O., & Çabas, B. M. (2021). Mathematical modelling of vacuum ohmic evaporation process. *Innovative Food Science and Emerging Technologies, 67*, Article 102560.

https://doi.org/10.1016/j.ifset.2020.102560

[21] Tao, Y., Yan, B., Zhang, N., Wang, M., Zhao, J., Zhang, H., Chen, W., & Fan, D. (2021). Microwave vacuum evaporation as a potential technology to concentrate sugar solutions: A study based on dielectric spectroscopy. *Journal of Food Engineering, 294*, Article 110414. https://doi.org/10.1016/j.jfoodeng.2020.110414

[22] Tao, Y., Yan, B., Zhang, N., Zhao, J., Zhang, H., Chen, W., & Fan, D. (2023). Decoupling thermal effects and possible non-thermal effects of microwaves in vacuum evaporation of glucose solutions. *Journal of Food Engineering, 338*, Article 111257. https://doi.org/10.1016/j.jfoodeng.2022.111257

[23] Tao, Y., Yan, B., Zhang, N., Zhao, J., Chen, W., & Fan, D. (2026). Microwave vacuum evaporation of sugar solutions: Analysis of dielectric and microwave absorption properties. *Journal of Food Engineering, 403*, Article 112728. https://doi.org/10.1016/j.jfoodeng.2025.112728

[24] Lata, S., Kumar, A., Kulshrestha, R., Chhetri, K. B., & Singh, D. (2025). Effects of changes in thermophysical and dielectric properties of pineapple juice on microwave power absorption density of the juice. *Food and Bioproducts Processing, 150*, 310-321. https://doi.org/10.1016/j.fbp.2025.01.020

[25] Burdo, O. G., Gavrilov, A. V., Sirotyuk, I. V., Ruzhitskaya, N. V., & Goncharov, D. S. (2022). Electrodynamic Apparatuses for Solutions' Concentration. *Surface Engineering and Applied Electrochemistry, 58 (3)*, 290–298. https://doi.org/10.3103/S1068375522030073

[26] Tian, S., Guo, L., Li, N., Yuwen, C., Xu, L., Guo, S., & Ju, S. (2024). Scientific basis and development trend of microwave heating enhanced flash evaporation process [微波加热强化闪蒸工艺的科学基础及发展趋势]. *Huagong Jinzhan/Chemical Industry and Engineering Progress, 43 (1)*, 135-144. https://doi.org/10.16085/j.issn.1000-6613.2023-1175

[27] Gavrilov, A. V., & Gerber, Y. U. B. (2023). Study of the features of modeling microwave vacuum evaporation. *BIO Web of Conferences, 78*, Article 06003. https://doi.org/10.1051/bioconf/20237806003

[28] Gavrilov, A. V., & Gerber, Y. B. (2024). Parameters of Modular Microwave Vacuum Evaporators [Параметры модульных микроволновых вакуум выпарных установок]. *Food Processing: Techniques and Technology, 54 (1)*, 135–145. https://doi.org/10.21603/2074-9414-2024-1-2495

[29] Hameed, A., Maan, A. A., Khan, M. K. I., Mahmood Khan, I., Niazi, S., Waheed Iqbal, M., Riaz, T., Manzoor, M. F., & Abdalla, M. (2023). Evaporation kinetics and quality attributes of grape juice concentrate as affected by microwave and vacuum processing. *International Journal of Food Properties, 26 (1)*, 1596–1611. https://doi.org/10.1080/10942912.2023.2218062

[30] Ibis, O. I., Bugday, Y. B., Aljurf, B. N., Goksu, A. O., Solmaz, H., Oztop, M. H., & Sumnu, G. (2024). Crystallization of sucrose by using microwave vacuum evaporation. *Journal of Food Engineering, 365*, Article 111847. https://doi.org/10.1016/j.jfoodeng.2023.111847

[31] Saengsuwan, T., & Sujinda, N. (2026). Hybrid mechanistic modeling of integrated enzymatic and vacuum processing for sustainable banana syrup production. *Applied Food Research, 6 (1)*, Article 101780. https://doi.org/10.1016/j.afres.2026.101780

[32] Jethi, G. S., Kushwaha, N., Sunori, S., & Juneja, P. (2026). Digital twin-based intelligent control system for sugar factory with reinforcement learning optimization. *Engineering Research Express, 8 (4)*, Article 045402. https://doi.org/10.1088/2631-8695/ae429b

[33] Asghar, M. T., Yusof, Y. A., Mokhtar, M. N., Yaacob, M. E., Ghazali, H. M., Varith, J., Chang, L. S., & Manaf, Y. N. (2020). Processing of coconut sap into sugar syrup using rotary evaporation, microwave, and open-heat evaporation techniques. *Journal of the Science of Food and Agriculture, 100 (10)*, 4012–4019. https://doi.org/10.1002/jsfa.10446

[34] Alizadeh, H. R., Mortezapour, H., Akhavan, H. R., & Balvardi, M. (2021). Physicochemical changes of barberry juice concentrated by liquid desiccant-assisted solar system and conventional methods during the evaporation process. *Journal of Food Science and Technology, 58 (11)*, 4370–4381.

https://doi.org/10.1007/s13197-020-04919-z

[35] Sujinda, N., Chaichana, N., Saengsuwan, T., & Varith, J. (2025). Optimization of Enzymatic Extraction and Vacuum-Assisted Evaporation Parameters for Banana Syrup Production. *International Journal of Food Science, 2025 (1)*, Article 8891536. https://doi.org/10.1155/ijfo/8891536

[36] Chedao, N., & Jehsu, A. (2026). Application of vacuum evaporation controlled by microcontroller for quality retention of stingless bee honey. *IOP Conference Series: Earth and Environmental Science, 1592 (1)*, Article 012038. https://doi.org/10.1088/1755-1315/1592/1/012038

[37] Rika, G. P., Maryam, & Dewi, H. (2020). Technical Analysis of Liquid Sugar Production Process of Raw Sago Starch Using the Enzymatic Hydrolisis Method of Pilot Plant Scale. *IOP Conference Series: Earth and Environmental Science, 515 (1)*, Article 012070. https://doi.org/10.1088/1755-1315/515/1/012070

[38] Julai, K., Sridonpai, P., Ngampeerapong, C., Tongdonpo, K., Suttisansanee, U., Kriengsinyos, W., On-Nom, N., & Tangsuphoom, N. (2023). Effects of Extraction and Evaporation Methods on Physico-Chemical, Functional, and Nutritional Properties of Syrups from Barhi Dates (Phoenix dactylifera L.). *Foods, 12 (6)*, Article 1268. https://doi.org/10.3390/foods12061268

[39] Tsygankov, S. P., Ivanova, T. S., Spivak, S. I., Lukashevich, K. M., & Blume, Y. A. B. (2024). Development of a complex technology for replacing fossil energy carriers with by-products in the bioethanol production [РОЗРОБЛЕННЯ КОМПЛЕКСНОЇ ТЕХНОЛОГІЇ ЗАМІЩЕННЯ ВИКОПНИХ ЕНЕРГОНОСІЇВ ПОБІЧНИ-МИ ПРОДУКТАМИ ВИРОБНИЦТВА БІОЕТАНОЛУ]. *Science and Innovation, 20 (5)*, 53–61. https://doi.org/10.15407/scine20.05.053

[40] Terki, L., Aissaoui, O., Hadjout, L., Calvini, R., Montevecchi, G., Khelouia, L., Baziz, H., Oukhmanou-Bensidhoum, S., Kaci, M., Boulekbache-Makhlouf, L., Kujawski, W., & Madani, K. (2025). Mathematical Modeling for Cactus Pear Juice Concentration Kinetics and a Study of the Physicochemical Changes During the Concentration Process. *Journal of Food Processing and Preservation, 2025 (1)*, Article 3124679. https://doi.org/10.1155/jfpp/3124679

[41] Kuşçu, A., & Bulantekin, Ö. (2021). Determination of phenolics, organic acids, minerals and volatile compounds of jujube (Ziziphus jujuba miller) jam produced by under vacuum evaporation compared with open pan method. *Journal of Food Measurement and Characterization, 15 (2)*, 1127–1138. https://doi.org/10.1007/s11694-020-00713-9

[42] Sabanci, S., & Icier, F. (2020). Rheological behavior of sour cherry juices concentrated by ohmic and conventional evaporation processes under vacuum. *Journal of Food Processing and Preservation, 44 (10)*, Article e14832. https://doi.org/10.1111/jfpp.14832

[43] Cochachin-Carrera, B., Moreno-Cuevas, J., & Carvajal-Mena, N. (2023). Effects of concentration by block freezing and vacuum evaporation on the physicochemical properties and digestibility of whey. *CYTA - Journal of Food, 21 (1)*, 313–320. https://doi.org/10.1080/19476337.2023.2196321